



Institute of Internet and Intelligent Technologies
Vilnius Gediminas Technical University
Saulėtekio al. 11, 10223 Vilnius, Lithuania
<http://www.isarc2008.vgtu.lt/>

**The 25th International Symposium
on Automation and Robotics in Construction**

June 26–29, 2008

ISARC-2008

ONLINE-ESTIMATION OF VIBRATORY DRIVEN PILES' BEARING CAPACITY: A FIRST APPROACH

Markus Schönit

Institute for Technology and Management in
Construction, University of Karlsruhe, Germany
schoenit@tmb.uni-karlsruhe.de

Dirk Reusch

Kybernetik Dr. Reusch
Pliezhausen, Germany
reusch@kybdr.de

ABSTRACT

Bearing capacity is an important attribute of driven piles. For centuries pile hammers have been used and their number of blows can be interpreted with respect to piles' bearing capacity and soil characteristics. However, currently no method exists to interpret process parameters of vibratory pile driving with respect to a pile's bearing capacity.

In a first step laboratory piling experiments using a vibrator and a hammer are carried out. The bearing capacities of the used model piles are determined by static load tests and secondary pile hammerings. In a second step large-scale piling experiments are carried out to enlarge and verify the results of the laboratory tests. For these experiments piles of different lengths have been driven using a diesel hammer and a vibrator. Apart from usual vibratory pile driving parameters the acceleration and the force between vibrator and clamping device were measured in realtime. Based on this data a specific driving energy can be determined and interpreted as a number of blows of a pile hammer. This allows the online-estimation of a vibratory driven pile's bearing capacity.

KEYWORDS

Bearing capacity, vibratory pile driving, diesel hammer, online-estimation

1. INTRODUCTION

Bearing capacity is one of the most important features of driven piles. Proof of a pile's bearing capacity can be furnished by static [1] or dynamic [2] pile tests. They are expensive and can be very time consuming in case of static load tests. For dynamic tests like CAPWAP¹ [3] one needs to be quite experienced in order to get trustworthy and reliable

results. Furthermore, data analysis is usually done well after physical testing, i.e. offline.

Very often a pile hammer's number of blows will be accepted as proof of the bearing capacity of a pile [4], [5]. When using a pile hammer this is a by-product at almost no additional cost. However, pile hammering comprises some disadvantages. It is high in noise, generates significant shock-stress and diesel hammers emit polluting exhaust fumes. All this can be avoided by using vibratory pile drivers instead of hammers.

¹ Case Pile Wave Analysis Program

In the last 10 years some research (e.g. [6], [7], [8], [9], [10]) has been undertaken in the area of vibratory pile driving. Nevertheless, in contrast to pile hammers there is currently no known and accepted quantity, like the number of blows, to prove the bearing capacity of a pile for vibratory pile drivers.

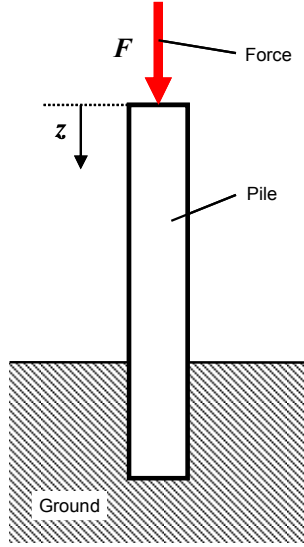


Figure 1: Piling Principle

2. PILING METHODS & DRIVING ENERGY

All piling methods are based on the same piling principle (Figure 1). A pile is driven into the ground (z -direction) by applying a driving force F on the pile head. We refer to the associated energy

$$E = \int_{z_0}^{z_1} F dz \quad (1)$$

as driving energy. It is the amount of energy transmitted into the pile (head) in order to achieve a penetration $\Delta z = z_1 - z_0$ of the pile. Thus

$$E_{\Delta z} = \frac{E}{z_1 - z_0} = \frac{E}{\Delta z} \quad (2)$$

will be called penetration-specific driving energy.

2.1. Pile Hammers

It is common practice to count the number of blows $N_{\Delta z}$ needed for a penetration Δz (e.g. N_{10} or N_{100} with $\Delta z = 10\text{cm}$ or 100cm). A simple hammer works like this: a mass m_h (hammer) is falling under gravity from a height h above the pile of mass m_p . When the hammer hits the pile a driving force is generated. Presuming rigid bodies, the efficiency of the impact shock is according to NEWTON given by

$$\eta = \frac{m_h + k^2 \cdot m_p}{m_h + m_p} \quad (3)$$

k denotes the shock coefficient². Thus every blow is equivalent to a driving energy

$$E_h = m_h \cdot g \cdot h \cdot \eta \quad (4)$$

g denotes the acceleration due to gravity. Let $\Delta z_{h,0}$ the irreversible penetration caused by a blow, then

$$E_{h,0} = \frac{E_h}{\Delta z_{h,0}} \quad (5)$$

is the penetration-specific driving energy of that blow.

2.2. Vibratory Pile Driver

A driving force generated by vibratory pile drivers can be described as

$$F(t) = F_v^*(t) + \bar{F}_v \quad (6)$$

Where $F(t)$ and $F_v^*(t)$ are periodic with frequency f (period $T = \frac{1}{f}$) and \bar{F}_v shall be the offset of $F(t)$.

Motion of the pile head is given by

$$z(t) = \underbrace{x(t)}_{\approx \hat{x} \cdot \sin(2 \cdot \pi \cdot f \cdot t)} + v \cdot t \quad (7)$$

for a sufficiently short observation period [10]. v is the global penetration velocity. Evaluation of the work integral (Equation (1)) over one oscillation cycle yields

² k depends on involved materials, e.g. $k \approx 0.6$ for steel/steel

$$\begin{aligned}
E_v &= \int_t^{t+T} (F_v^*(t) + \bar{F}_v) \cdot (\dot{x}(t) + v) dt = \\
&\dots = \underbrace{\int_t^{t+T} F_v^*(t) \cdot \dot{x}(t) dt}_{E_v^*} + \underbrace{\frac{v}{f} \cdot \bar{F}_v}_{\bar{E}_v}.
\end{aligned} \quad (8)$$

E_v^* has to be performed by the vibrator and \bar{E}_v is due to the static load \bar{F}_v . Analogue to Equation (5) and with $\Delta z_{v,0}$ as the irreversible penetration:

$$\Delta z_{v,0} = \frac{v}{f}, \quad (9)$$

$$E_{v,0} = \frac{E_v}{\Delta z_{v,0}} = \frac{f}{v} \cdot \int_t^{t+T} F_v^*(t) \cdot \dot{x}(t) dt + \bar{F}_v \quad (10)$$

resembles the penetration-specific driving energy performed over an oscillation cycle.

3. LABORATORY EXPERIMENTS

Laboratory experiments were carried out using a pile hammer and a vibratory pile driver. Penetration-specific driving energies $E_{h,0}$ and $E_{v,0}$ of both piling methods were measured and will be compared quantitatively.

3.1. Soil, Pile and Pile Drivers

Two different granular cohesionless soils were used. In the following, they are called fine and coarse soil (Table 1). A pile (Table 2) was driven at different depths (20, 30, 40, 50 and 60cm) either with a pile hammer (Figure 2a, Table 3) or with a vibratory pile driver (Figure 2b, Table 3). Acceleration \ddot{z} of the pile head and driving force F were measured.

3.2. Static Load Tests

Each driven pile was static load tested. For example, Figure 3 shows typical load-settlement curves of vibratory (30Hz) driven piles. For our purposes, we define bearing capacity as a load which provokes a settlement of 5mm (see solid horizontal line in Figure 3).

Table 1: Soil Characteristics (Laboratory)

	Fine	Coarse
Grain Size:	0...0.5mm	0.5...2mm
Density Index:	0.90	0.68
Water Content:	0.12%	0.01%
Density of Grain:	2.66g/cm ³	2.60g/cm ³
Density (in situ):	1.58g/cm ³	1.63g/cm ³

Table 2: Pile Specifications (Laboratory)

Type:	H-Profile (60x60x5mm)
Material:	Aluminium
Length:	111.7mm
Mass:	3.62kg
Pile Helmet:	1.58kg (Steel/Aluminium)

Table 3: Pile Driver Specifications (Laboratory)

Pile Hammer	
Mass:	5.72kg
Height of Fall:	35 / 45cm
Potential Energy:	19.6 / 25.3Nm
Driving Energy:	9.6 / 12.3Nm
Vibratory Pile Driver	
Frequency:	20 / 25 / 30 / 35 / 40Hz
Static Moment:	0...0.125kgm
Surcharge Load:	0...900N
Dynamic Mass:	32kg



(a) Hammer

(b) Vibrator

Figure 2: Pile Drivers (Laboratory)

Bearing capacities (5mm settlement) of all piles driven into coarse soil are shown in Figure 4. At the same depth all piles exhibit approximately ($\pm 15\%$) the same bearing capacity. The greater the depth is the greater is the bearing capacity. Similar results were obtained for experiments in fine soil.

Load vs. Settlement of Vibratory Driven Piles (30Hz, Coarse Soil)

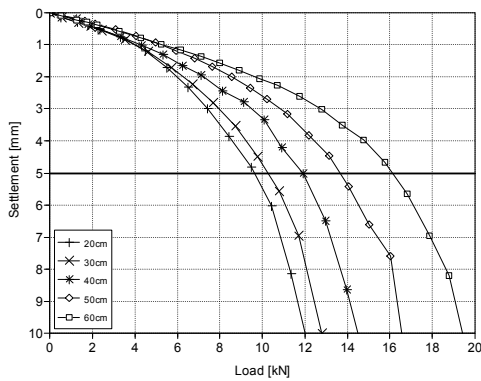


Figure 3: Static Load Tests of Vibratory Driven Piles

3.3. Secondary Pile Hammering

It was expected that the piling process would compact or loosen up the soil. Thus the bearing capacity of a pile would not be independent of the piling method and its parameters [11]. Indirect confirmation of that was achieved by secondary pile hammering experiments. At first we drove a pile by vibration (20, 30 or 40Hz) at a preliminary depth (30 or 40cm) and then secondly we used hammering to increase the piling depth at least by 5cm. Secondary hammering was then compared with a reference pile (driven only by hammer). If $E_{h,0}$ (or $\Delta z_{h,0}$) of both are differing significantly then vibratory pile driving changed the soil characteristics in a different way in comparison to pile hammering.

Results of such an experiment are shown in Figure 5. At a depth of 30cm we get $E_{h,0} \approx 32 \text{ Nm/cm}$ for the reference pile and a significantly higher value $E_{h,0} \approx 43 \text{ Nm/cm}$ for secondary pile hammering. For this example, we can conclude that vibratory pile driving leads to a more compacted soil compared to pile hammering.

Bearing Capacity (Settlement 5mm) vs. Piling Depth (Coarse Soil)

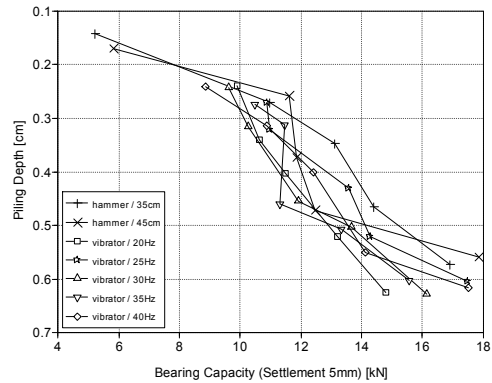


Figure 4: Bearing Capacities in Coarse Soil

Driving Energy vs. Piling Depth (Fine Soil)

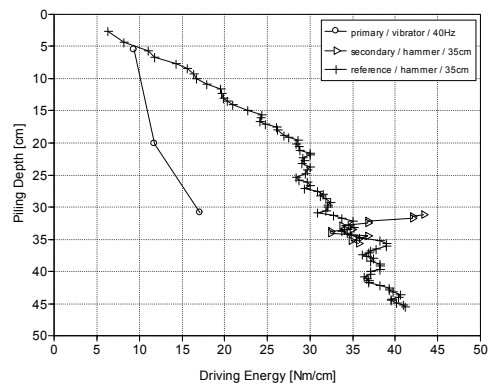


Figure 5: Secondary Pile Hammering Experiment

3.4. Comparison of Driving Energies

First (case A) we can compare $E_{v,0}$ of vibratory driven piles with $E_{h,0}$ of reference piles (driven only by hammer) at the same depth, i.e. approximately ($\pm 15\%$) the same bearing capacity (cp. Figure 4). Data of experiments in coarse soil are shown in Figure 6. We find that $E_{v,0} \leq E_{h,0}$ at the same depth. Both $E_{v,0}$ and $E_{h,0}$ are increasing with increasing depth. Data of vibratory pile drives are more scattered and it seems that $E_{v,0}$ depends on the vibration frequency. Secondly (case B) we can compare $E_{v,0}$ with $E_{h,0}$ of secondary pile hammerings (cp. Figure 5).

We define an energy ratio

$$\varepsilon = \frac{E_{v,0}}{E_{h,0}} \quad (11)$$

to facilitate further data analysis and interpretation. ε was computed for both cases (ε_A and ε_B) and different vibration frequencies. Results are shown in Figure 7. In fine and coarse soil we have $\varepsilon_A \approx 0.6$ and there seems to be a slight decrease of ε_A towards higher frequencies. Regarding ε_B , we find it clearly dependent on frequency, i.e. $\varepsilon_B = \varepsilon_B(f)$, and $\varepsilon_B \leq \varepsilon_A$.

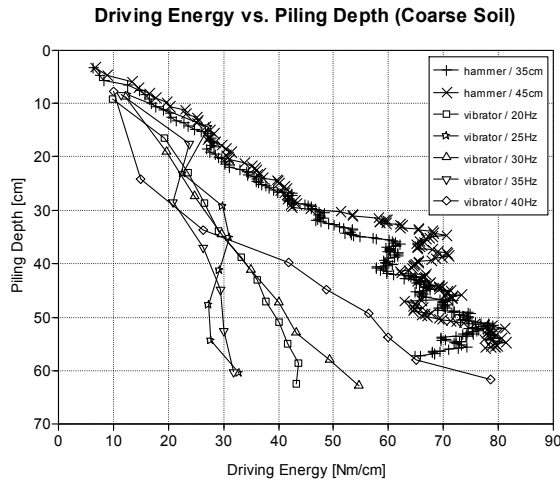


Figure 6: Driving Energy in Coarse Soil

3.5. Estimation Scheme for Number of Blows

The driving Energy $E_{v,0}$ of vibratory pile driving could be determined online and interpreted as number of blows

$$N_0 = \frac{1}{\Delta z_{h,0}} = \frac{E_{v,0}}{\varepsilon \cdot E_h} \quad (12)$$

of an arbitrary pile hammer. For this, the energy per blow E_h and the energy ratio ε (cp. Equation (11)) must be known. We used Equations (3) and (4) to determine E_h and found very good correspondence with our measurements. Under laboratory conditions, ε was determined empirically and found to be dependent on frequency (cp. Sec. 3.4).

4. LARGE-SCALE EXPERIMENTS

Large-scale experiments were carried out at the test site of the Institute for Technology and Management in Construction near Karlsruhe (soil characteristics are described in [6] and [7]). Piles were driven by vibration and subsequently tested by pile hammering (cp. Sec. 3.3). For reference, piles were also driven by hammer only.

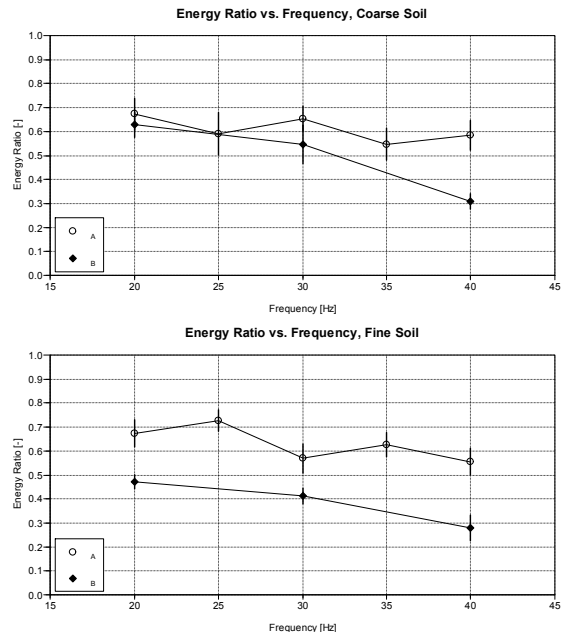


Figure 7: Energy Ratio ε

4.1. Realtime Data Acquisition

Apart from obvious parameters (frequency, static moment, piling depth, etc.), the acceleration of the vibrator and the force between vibrator and clamping device were measured. The realtime data acquisition was accomplished using PC/104 hardware [12] running Linux with the realtime extension RTAI [13] and COMEDI [14]. Captured and evaluated data was sent every second to another computer for visualisation and archiving. This was done over a TCP/IP-connection using SOAP [15].

4.2. Piles and Pile Drivers

PEINER PSp 370 piles of different lengths were used (Table 4). They were driven by a MÜLLER MS-10

HFV vibrator (Table 5, Figure 9) and a DELMAG D12-32 diesel hammer (Table 5, Figure 8).

Table 4: Pile Specifications (Large-Scale)

Type:	PEINER PSp 370
Material:	Steel
Length:	5.5 / 7.5 / 9.5m
Mass:	671 / 915 / 1159kg
Pile Helmet:	610kg (Steel/Plastic)



Figure 8: Diesel Hammer

Table 5: Pile Driver Specifications (Large-Scale)

Pile Hammer (DELMAG D12-32)	
Impact Mass:	1280kg
Diesel Injection per Stroke:	2,10cm ³
Potential Energy per Stroke:	42460Nm
Frequency:	36...52 Strokes/min
Vibratory Pile Driver (MÜLLER MS-10 HFV)	
Frequency:	0...39.3Hz
Static Moment:	0...10kgm
Dynamic Mass:	1700kg
Clamping Device:	770kg



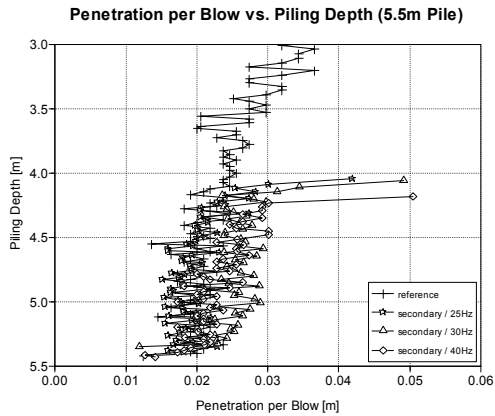
Figure 9: Vibratory Driver

4.3. Secondary Hammering Results

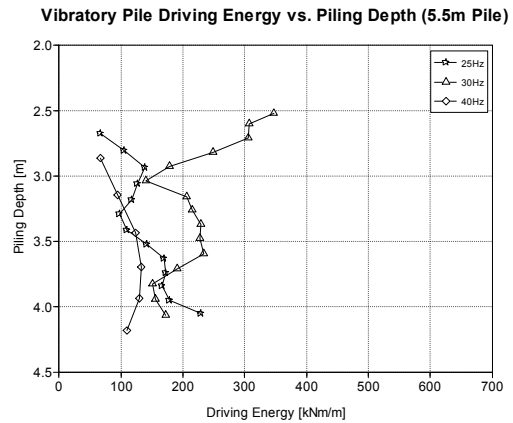
Penetrations per blow $\Delta z_{h,0}$ are presented in Figure 10 as a result of secondary hammering. If we assume the diesel hammer's impact to be constant³, then they are in inverse proportion to the penetration-specific driving energies $E_{h,0}$ (cp. Equation (5)). With short (5.5m) piles at a depth of about 4m (Figure 10a) we initially have $\Delta z_{z,0}=0.04\dots0.05\text{m}$, which is significantly greater than $\Delta z_{z,0}\approx 0.025\text{m}$ of the reference pile. This difference vanishes after a few blows. With long (9.5m) piles at the depth of about 8m (Figure 10b) there is no such big difference between secondary hammering and the reference pile.

The determination of the driving energy which is transmitted into the pile's head by the diesel hammer is much more complicated than for the simple hammer at the laboratory experiments. Thus the hammering driving energy will be presented on the next pages but the detailed determination will be illustrated in a future publication.

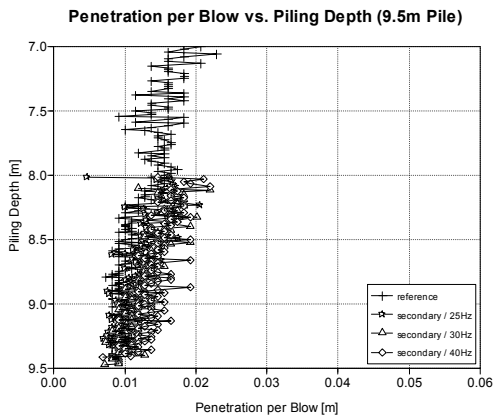
³ In practice diesel hammers are working with $\eta\approx 0.5\dots 0.7$ [16] and it is known that η depends on the frequency of blows. This issue will be addressed in a future publication.



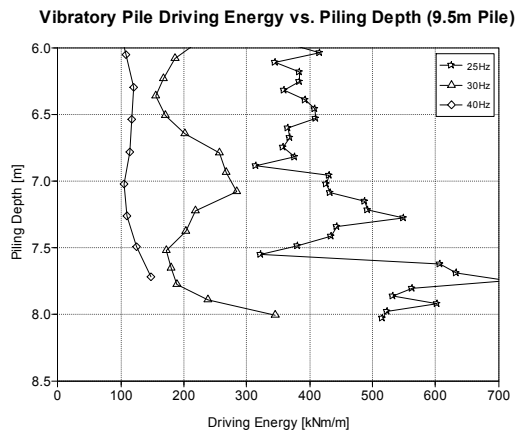
(a) Short Pile (5.5m)



(a) Short Pile (5.5m)



(b) Long Pile (9.5m)



(b) Long Pile (9.5m)

Figure 10: Secondary Hammering Results

Figure 11: Vibratory Pile Driving Energy $E_{v,0}$

4.4. Vibratory Pile Driving Energy

Prior to the above mentioned secondary hammering, piles were driven by vibration. The respective driving energies $E_{v,0}$ are shown in Figure 11. The data series are smoothed by using moving average over three data points. When short (5.5m) piles are driven with 40Hz, $E_{v,0}$ is lower than at the frequencies of 25 and 30Hz (Figure 11a). For the long piles (9.5m) it is clearer that $E_{v,0}$ heavily depends on the vibration frequency (Figure 11b). $E_{v,0}$ at 25Hz is approximately four times higher than at 40Hz. The higher the frequency is, the lower $E_{v,0}$ is.

4.5. Applicability of Vibratory Pile Driving Energy

As it is shown in Figure 11 the curves of the vibratory driving energy are subjected to a very wide distribution which is much more marked than in the laboratory experiments (cp. Sec. 3.4). Caused by this spread of data a comparison of penetration-specific vibratory driving energy and penetration-specific hammering driving energy seems not reasonable.

So it is necessary to take a closer look at the vibratory driving energy and therefore especially at the motion of a pile.

4.6. Vibratory Pile Driving Energy - Toe Contact

The energy which is transmitted by the vibrator into the pile's head is dissipated differently. On the one hand the energy is consumed for overcoming the shaft resistance while the pile is penetrating the soil. On the other hand the energy is necessary for overcoming the toe resistance when the pile is moving downwards and the pile's toe has contact with the soil. This part of energy is responsible for the irreversible penetration and so it seems to be reasonable to consider especially this part of energy for the comparison with the pile driving energy of the hammer.

This part of the vibratory pile driving energy can be approximately calculated with

$$E_{vt} = \int_{t_1}^{t_2} (F_v^*(t) + \bar{F}_v) \cdot (\dot{x}(t) + v) dt = \dots = \int_{t_1}^{t_2} F_v^*(t) \cdot \dot{x}(t) dt + \frac{v}{f} \cdot \bar{F}_v. \quad (13)$$

t_1 and t_2 denote the limits of the time interval in which the pile makes a downward motion and the pile's toe has contact with the soil. t_1 and t_2 can be determined on the basis of the pile motion. Figure 12 shows the pile motion during one oscillation cycle.

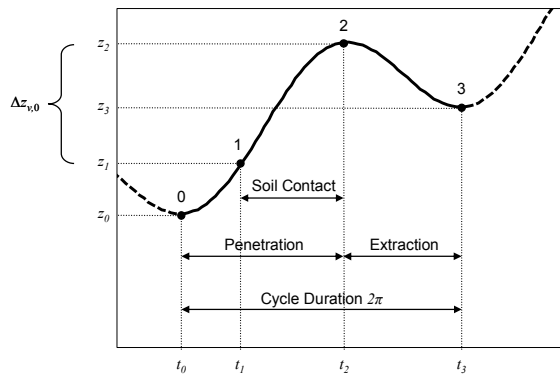


Figure 12: Pile Motion

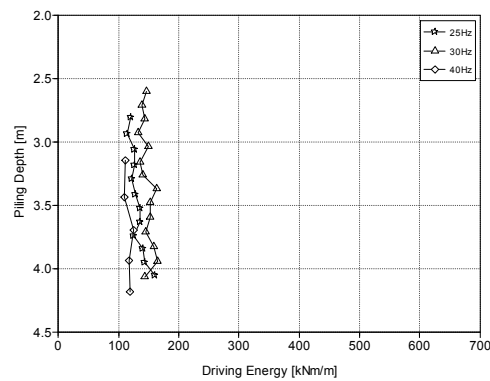
t_2 is defined as that point of time when the pile's toe has reached the reversal point z_2 . t_1 , that is the point of time when the toe's contact with the soil begins and can be determined when z_1 is known:

$$z_1 = z_2 - \Delta z_{v,0}. \quad (14)$$

Analogue to Equation (10), it is possible to determine the penetration-specific driving energy when the toe has soil contact:

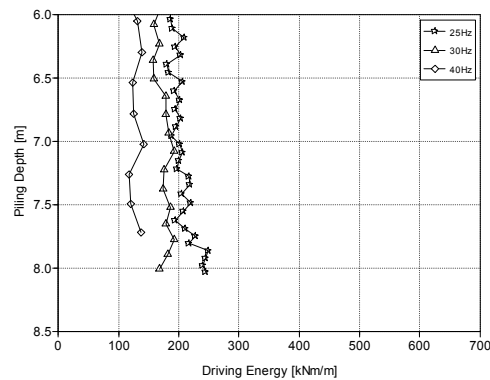
$$E_{vt,0} = \frac{E_{vt}}{\Delta z_{v,0}} = \dots = \frac{f}{v} \cdot \int_{t_1}^{t_2} F_v^*(t) \cdot \dot{x}(t) dt + \bar{F}_v. \quad (15)$$

Vibratory Pile Driving Energy (Toe Contact) vs. Piling Depth (5.5m Pile)



(a) Short Pile (5.5m)

Vibratory Pile Driving Energy (Toe Contact) vs. Piling Depth (9.5m Pile)



(b) Long Pile (9.5m)

Figure 13: Vibratory Pile Driving Energy $E_{vt,0}$

Figure 13 shows the vibratory pile driving energy $E_{vt,0}$ for short and long piles. When short piles (5.5m) are driven with a vibration frequency of 40Hz, $E_{vt,0}$ is

lower than at the frequencies of 25 and 30Hz (Figure 13a). For the long piles (9.5m) it is similar to the short piles. $E_{vt,0}$ depends on the vibration frequency (Figure 13b), the higher the frequency is, the lower is $E_{vt,0}$. $E_{vt,0}$ at the frequency of 25Hz is about 50% higher than at 40Hz. In contrast to Figure 11, where the complete driving energy which is performed over the full oscillation cycle $E_{v,0}$ is shown, the curves of $E_{vt,0}$ do not differentiate so significantly.

4.7. Comparison of Driving Energies

$E_{vt,0}$ seems to be a useful parameter for the comparison with hammering driving energy. But with regard to the secondary hammering results, especially to the penetrations per blow $\Delta z_{h,0}$ (Figure 10), it seems reasonable to average the penetration-specific energy over 10cm to decrease the influence of single blows. Therefore we get the averaged energy for vibratory driven piles

$$E_{vt,10} = \frac{1}{0.1m} \cdot \int_{z_n-0.1m}^{z_n} E_{vt,0}(z) dz \quad (16)$$

and for hammering driven piles

$$E_{h,10} = \frac{1}{0.1m} \cdot \int_{z_n-0.1m}^{z_n} E_{h,0}(z) dz. \quad (17)$$

Figure 14 shows the driving energy $E_{h,10}$ and $E_{vt,10}$ for long piles. $E_{h,10}$ of the used diesel hammer (Table 5) is more than five times higher than $E_{vt,10}$. At the data of $E_{h,10}$ a dependence of the vibration frequency is not recognisable. The curves of $E_{vt,10}$ most closely correspond to the curves of $E_{vt,0}$.

Analogue to Equation (11), we define the energy ratio

$$\varepsilon = \frac{E_{vt,10}}{E_{h,10}} \quad (18)$$

for the large-scale piles. ε was computed for different vibration frequencies. Figure 15 shows the results. As like the laboratory experiments before, ε depends on vibratory frequency, ε at 40Hz is lower than at 25Hz.

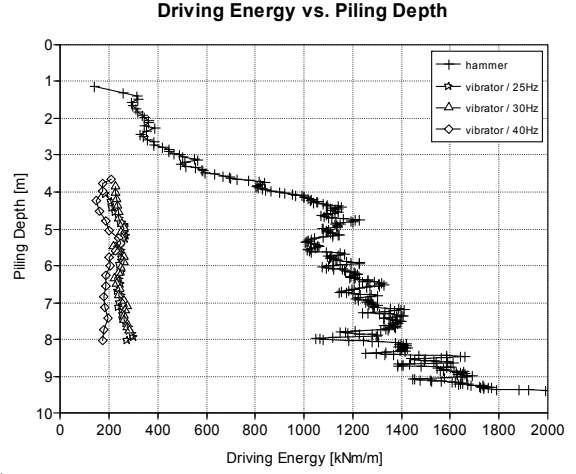


Figure 14: Driving Energy $E_{h,10}$ and $E_{vt,10}$

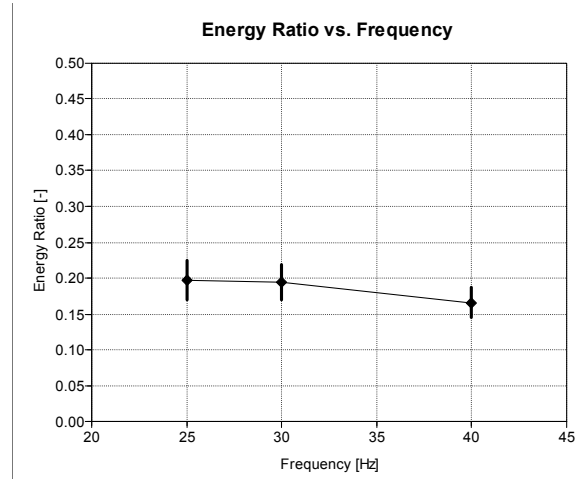


Figure 15: Energy Ratio ε

4.8. Estimation Scheme for Number of Blows

Analogue to the laboratory experiments before, the driving energy of the vibratory pile driver could be determined online. That part of driving energy which is decisive for the irreversible penetration can be estimated and interpreted as number of blows of an arbitrary pile hammer:

$$N_0 = \frac{1}{\Delta z_{h,0}} = \frac{E_{vt,0}}{\varepsilon \cdot E_h}. \quad (19)$$

5. CONCLUSION & FUTURE WORK

Laboratory experiments showed that online-estimation of vibratory driven piles' bearing capacity is principally possible. Based on measured data of the vibratory pile driving process and an empirically energy ratio, the vibratory pile driving energy can be interpreted as a number of blows of a pile hammer. Additional experiments in large scale should validate the results of the laboratory experiments. The large-scale experiments which were carried out in gravely sand showed that the penetration-specific driving energy varies immensely. Therefore, a new parameter for the comparison of vibratory pile driving with hammering pile driving was derived. This new parameter allows estimating that part of driving energy is responsible for the irreversible penetration of the vibratory driven pile. With this parameter and an empirically energy ratio it is possible, analogue to the laboratory experiments before, to interpret the decisive part of vibratory pile driving energy as a number of blows of a pile hammer.

This makes it principally possible to get an online-estimation of the vibratory driven piles' capacity on the construction site comparable with the driving record of a hammering driven pile.

Future work should be the data extension in different soils. Thereby the energy ratio ε can be approved and extended for different soil specifications. Furthermore, additional experiments should be carried out with different pile sections and greater pile lengths. At this it can be possible to come to the realisation that the presented method is not usable for very long piles (>30m).

6. ACKNOWLEDGEMENTS

The authors appreciate the financial support by the German Federal Ministry of Economics (Programme ProInno; Project-Nr. KF 0396601KPK2), the Ministry of Science, Research and Arts of Baden-Württemberg, and the cooperation with our industry partners ELPRO Verkehrstechnik GmbH, Berlin and THYSSENKRUPP GfT Tiefbautechnik GmbH, Alsfeld. Furthermore we would like to thank Mr. Stefan MEWES (DELMAG GmbH & Co. KG, Esslingen) for his valuable advice.

REFERENCES

- [1] Ellner, A., Linder, W.-R., et al.: *Empfehlungen für statische axiale Pfahlprobebelastungen*, Deutsche Gesellschaft für Geotechnik, Arbeitskreis 2.1, Essen, 1993.
- [2] Balthaus, H.: *Zur Bestimmung der Tragfähigkeit von Pfählen mit dynamischen Prüfmethode*, PhD thesis, Technische Universität Braunschweig, 1986.
- [3] Rausche, F., Goble, G. G., Likins, G. E. Jr.: *Dynamic determination of pile capacity*, Journal of Geotechnical Engineering, vol. 111, no. 3, pp. 367–383, 1985.
- [4] Deutsches Institut für Normung e.V., Berlin: *DIN 4026 Rammpfähle - Herstellung, Bemessung und zulässige Belastung*, August 1975.
- [5] Deutsches Institut für Normung e.V., Berlin: *DIN 4026 Rammpfähle – Herstellung, Bemessung und zulässige Belastung*, Oktober 1994.
- [6] Dierssen, G.: *Ein bodenmechanisches Modell zur Beschreibung der Vibrationsrammung in körnigen Böden*, PhD thesis, Universität Karlsruhe, 1994.
- [7] Oleff, A.: *Auslegung von Stellelementen für Schwingungserregerzellen mit geregelter Parameterverstellung und adaptive Regelungskonzepte für den Vibrationsrammprozeß*, PhD thesis, Universität Karlsruhe, 1996.
- [8] Cudmani, R. O.: *Statische, alternierende und dynamische Penetration in nichtbindigen Böden*, PhD thesis, Universität Karlsruhe, 2000.
- [9] Reusch, D.: *Automatic controlled vibratory pile driving with shock-stress limitation*, in Proc. of the 17th ISARC Int. Symp. on Automation and Robotics in Construction, 18-20 Sept., Taipei, Taiwan, pp. 905–910, 2000.
- [10] Reusch, D.: *Modellierung, Parameterschätzung und automatische Regelung mit Erschütterungsbegrenzung für das langsame Vibrationsrammen*, PhD thesis, Universität Karlsruhe, 2001.
- [11] Hartung, M.: *Einflüsse der Herstellung auf die Pfahltragfähigkeit in Sand*, PhD thesis, Technische Universität Braunschweig, 1994.
- [12] “PC/104 Embedded PC Modules“ <http://www.pc104.org>.
- [13] “DIAPM RTAI – Realtime Application Interface.” <http://www.aero.polimi.it/rtai/>.
- [14] “Comedi – The Linux Control and Measurement Interface.” <http://www.comedi.org>.
- [15] “gSOAP: SOAP C++ Web Services.” <http://gsoap2.sourceforge.net>.
- [16] Rausche, F.: *Pile driving equipment: Capabilities and properties*, in Proc. of the 6th Int. Conf. on the Application of Stresswave Theory to Piles, Sao Paulo, 2000.